SUPPORTING INFORMATION

Coordination and Conformational Isomers in Mononuclear Iron Complexes with Pertinence to the [FeFe] Hydrogenase Active Site

Andreas Orthaber,[a,‡] Michael Karnahl,[a,‡,#] Stefanie Tschierlei,[a,§] Daniel Streich,[a] Matthias Stein,[b,*] and Sascha Ott[a,*]

[a] Department of Chemistry, Ångström Laboratory, Uppsala University, Box 523, 75120 Uppsala, Sweden.
[b] Max-Planck-Institute for Dynamics of Complex Technical System, Sandtorstr. 1, 39106 Magdeburg, Germany.

Supporting Information – Table of Content:

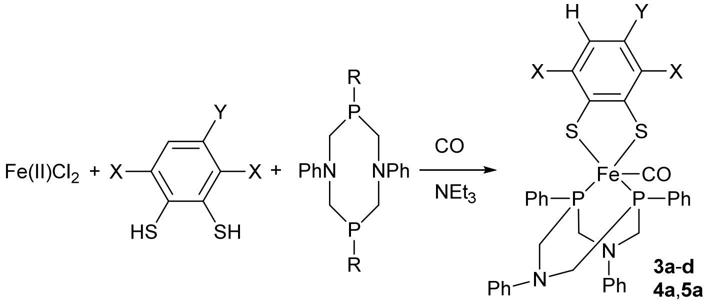

3a-d
4a,**5a**

Scheme ESI-1. Synthesis of penta coordinate complexes **3a-d** (X=Y=H), **4a** (X=Cl, Y = H), and **5a** (X= H, Y = CH_3). **a**: R= Ph, **b**: R = benzyl, **c**: R = *cyclo*-hexyl, **d** R = *tert.*-butyl.

Table ESI-1. Crystallographic data and refinement details for complexes **3a** and **3c**.

	P^{cyc}N^{Ph}	**3a** (R = phenyl)	**3c***CH_2Cl_2 (R= *cyclo*-hexyl)
Empirical formula	$C_{30}H_{32}N_2P_2$	$C_{35}H_{32}FeN_2OP_2S_2$	$[C_{35}H_{44}FeN_2OP_2S_2]_2$ $*[CH_2Cl_2]_2$
Formula weight [g mol^{-1}]	482.52	678.54	1551.11
CCDC-No.	972156	822967	972155
Crystal system	Orthorhombic	Monoclinic	Monoclinic
Space group	Pba2	*P2$_1$*/n	*P2$_1$*/c
Unit cell dimensions a[Å]	9.3653(2)	10.4473(5)	17.700(8)
b [Å]	26.2717(7)	17.7556(9)	17.198(8)
c [Å]	5.22710(10)	17.6965(9)	24.263(12)
α, β, γ [°]	90, 90, 90	90, 98.062(1), 90	90, 97.888(7), 90
Volume [Å^3], Z	1286.09(5), 2	3250.2(3), 4	7316(6), 4
Density [g cm^{-3}]	1.246	1.387	1.408
μ(MoK$_\alpha$) [mm^{-1}]	0.190	0.722	0.792
F(000)	512	1408	3248
Crystal size [mm]	0.6 x 0.3 x 0.3	0.33 x 0.25 x 0.13	0.13 x 0.11 x 0.05
Crystal Description	Colorless block	Green plates	Green block
Temperature [K]	100(2)	100(2)	100(2)
Radiation [Å]	0.71073	0.71073	0.71073
Θ range min, max [°]	2.31 - 26.39	2.28 - 28.82	1.161 - 26.000
Index ranges	$-11 \leq h \leq 11$, $-32 \leq k \leq 27$, $-6 \leq l \leq 6$	$-15 \leq h \leq 15$, $-23 \leq k \leq 25$, $-25 \leq l \leq 25$	$-21 \leq h \leq 21$, $-21 \leq k \leq 21$, $-29 \leq l \leq 29$
Reflections collected	6851	62319	103410
Reflections unique,	2584	9995	14381
Parameters, restraints	154, 1	388, 0	829
Flack parameter	0.01(9)	-	-
R(int)	0.0335	0.0655	0.3324
S	1.039	0.967	0.998
R_1 [$I > 2\sigma(I)$]	0.0306	0.0418	0.1094
wR_2 (all data)	0.0791	0.1183	0.3151
larges difference peak/hole [e A^{-3}]	0.256 / -0.150	1.396 / -0.364	1.899 / -1.222

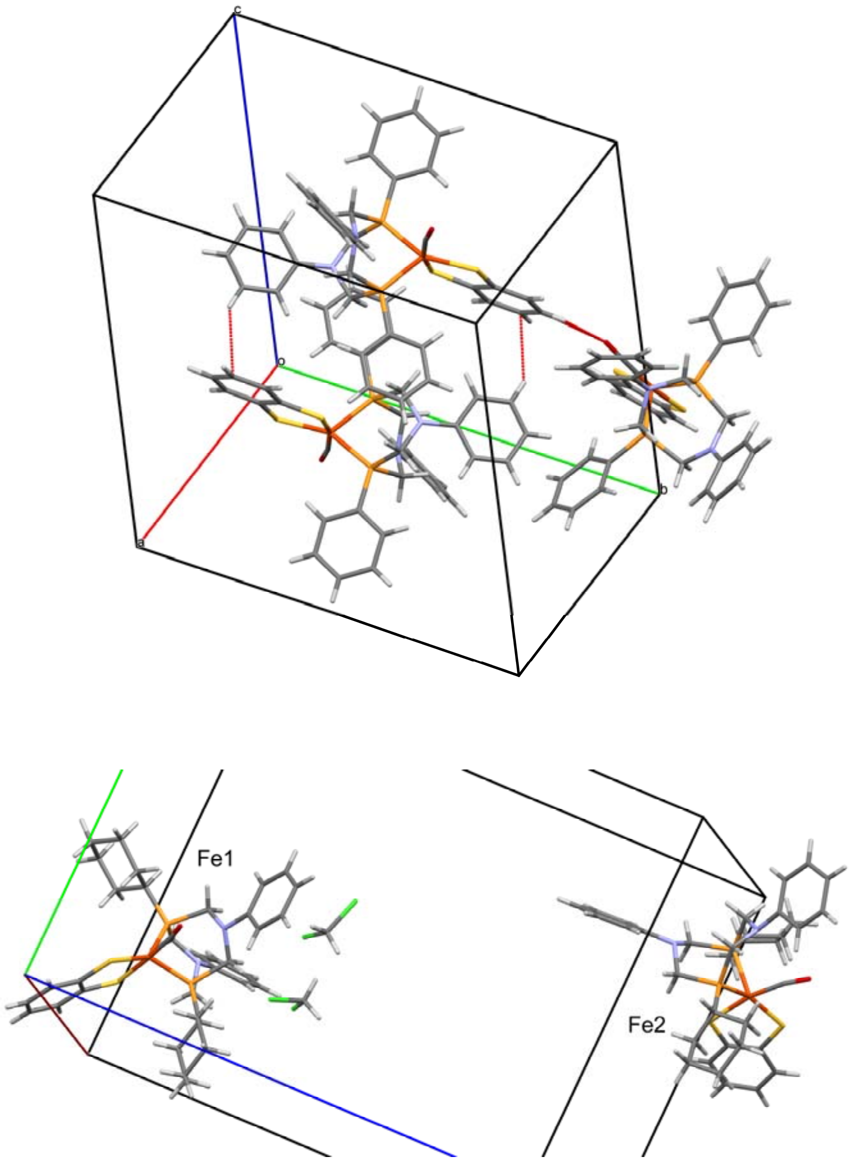

Figure ESI-1. Top: Molecular packing of **3a** indicating significant C-H···π interactions. (red dotted line). Bottom: Molecular packing of the independent units containing Fe1 and Fe2 of **3c** including the DCM solvates.

NMR data of the complexes 2, 3a-d, 4a and 5a.

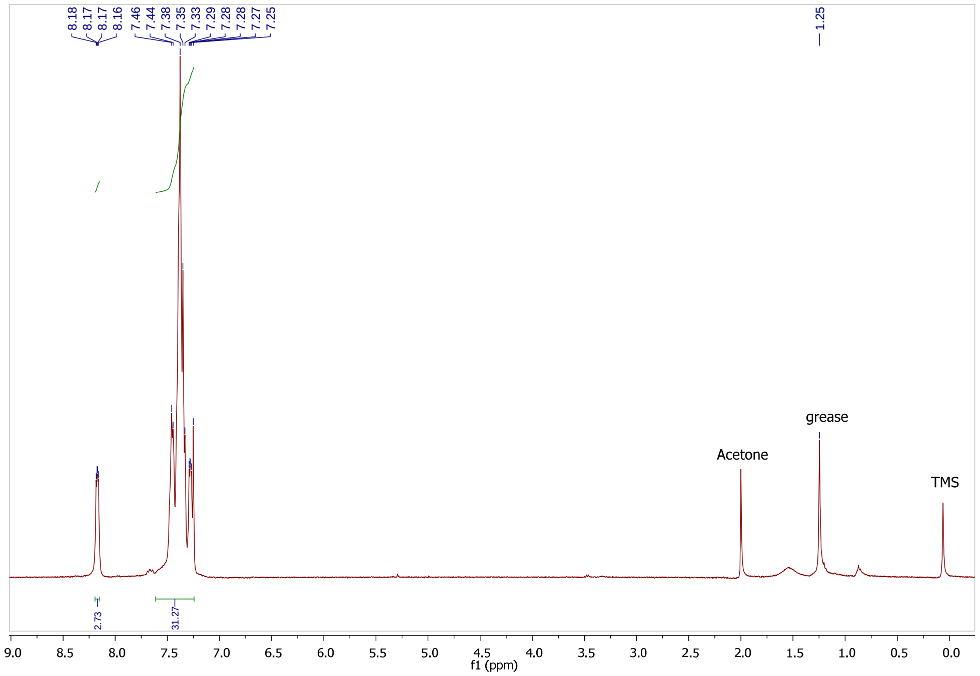

Figure ESI-2. . ^{1}H-NMR spectrum (400 MHz, $CDCl_3$) of complex [Fe(μ-bdt)$(PPh_3)_2(CO)_2$] **2**

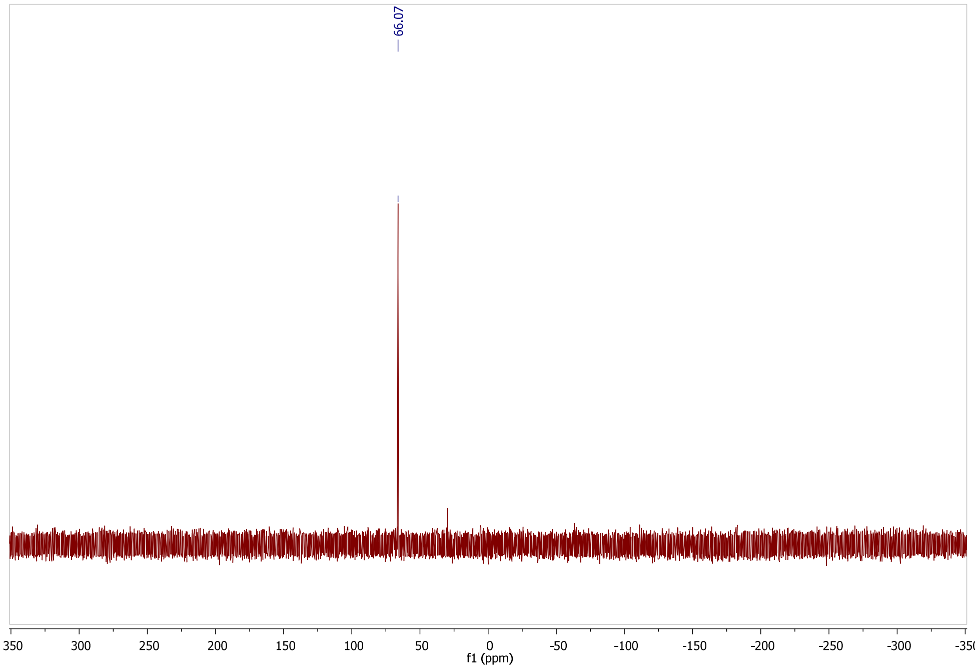

Figure ESI -3. $^{31}P\{^1H\}$-NMR spectrum (168 MHz, $CDCl_3$) of complex [Fe(μ-bdt)$(PPh_3)_2(CO)_2$] (**2**)

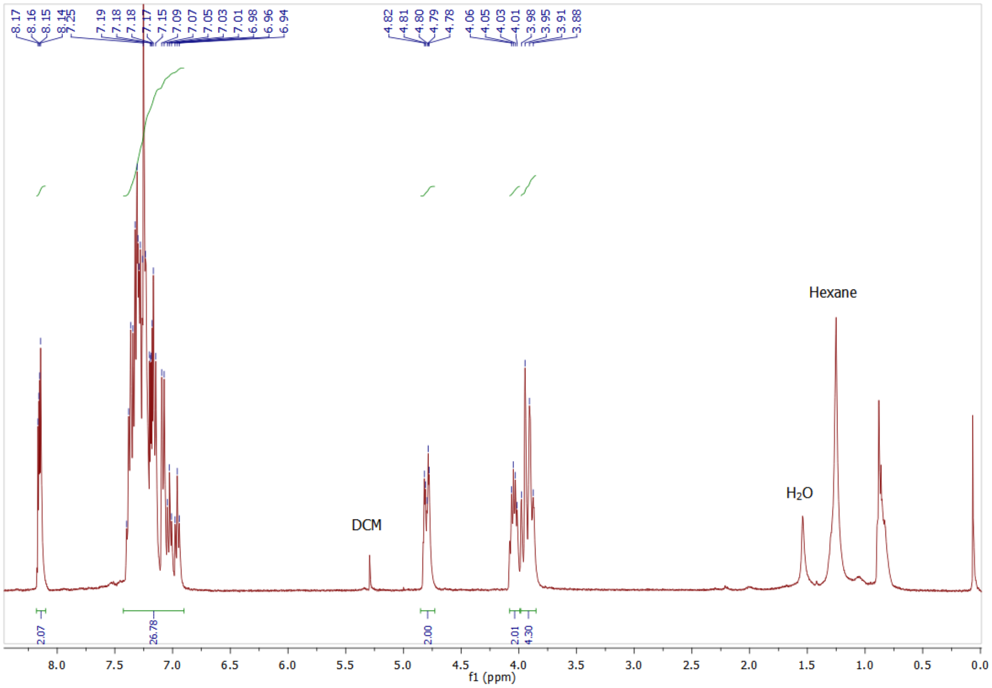

Figure ESI -4. ^{1}H-NMR spectra (400 MHz, $CDCl_3$ solution) of complex [Fe(μ-bdt)($P^{Ph}{}_2N^{Ph}{}_2$)(CO)] **(3a)**

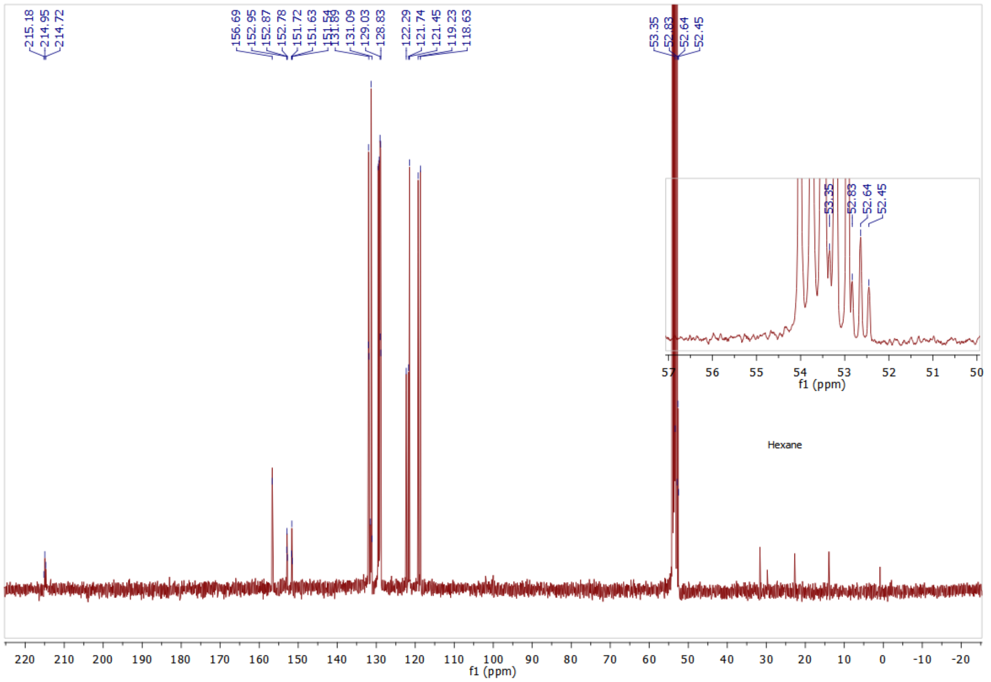

Figure ESI -5. $^{13}C\{^1H\}$-NMR spectrum (75.5 MHz, CD_2Cl_2 solution) of complex [Fe(μ-bdt)($P^{Ph}{}_2N^{Ph}{}_2$)(CO)] **3a**.

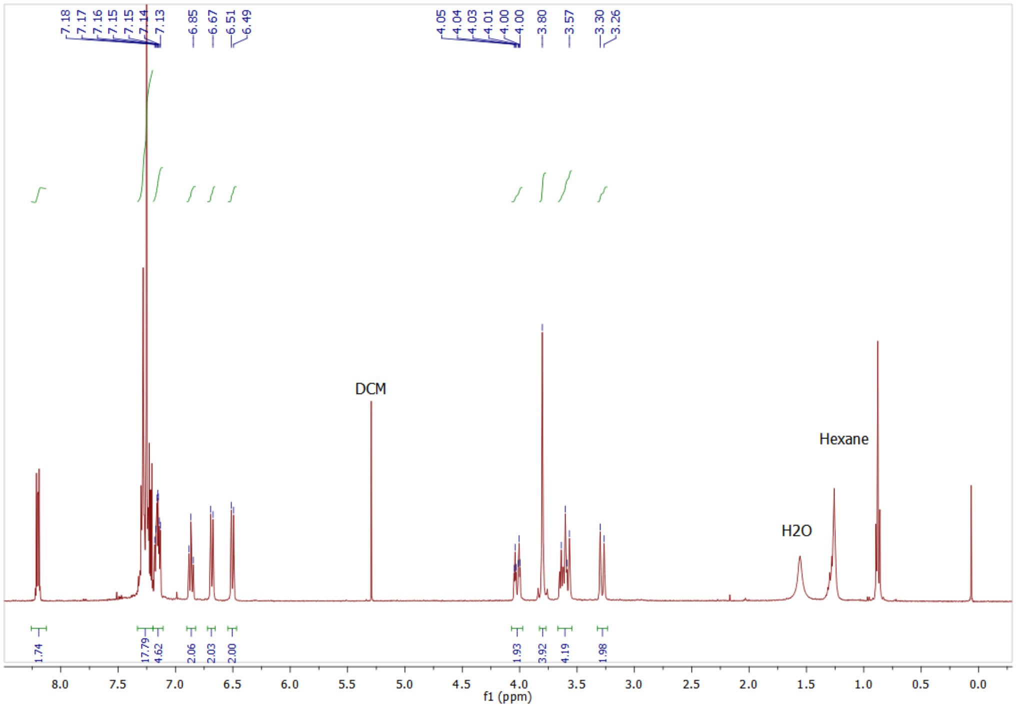

Figure ESI -6. ^{1}H-NMR spectra (400 MHz, $CDCl_3$ solution) of complex [Fe(μ-bdt)($P^{Bn}{}_2N^{Ph}{}_2$)(CO)] **3b** (Bn = benzyl).

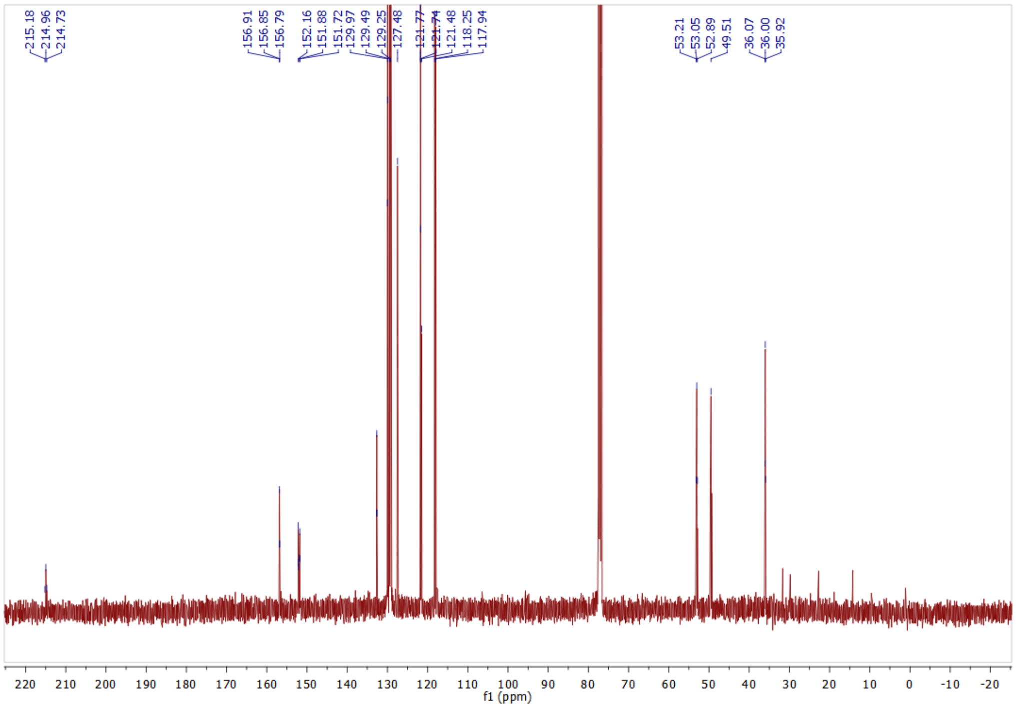

Figure ESI -7. $^{13}C\{^{1}H\}$-NMR spectrum (75.5 MHz, $CDCl_3$ solution) of complex [Fe(μ-bdt)($P^{Bn}{}_2N^{Ph}{}_2$)(CO)] **3b** (Bn = benzyl).

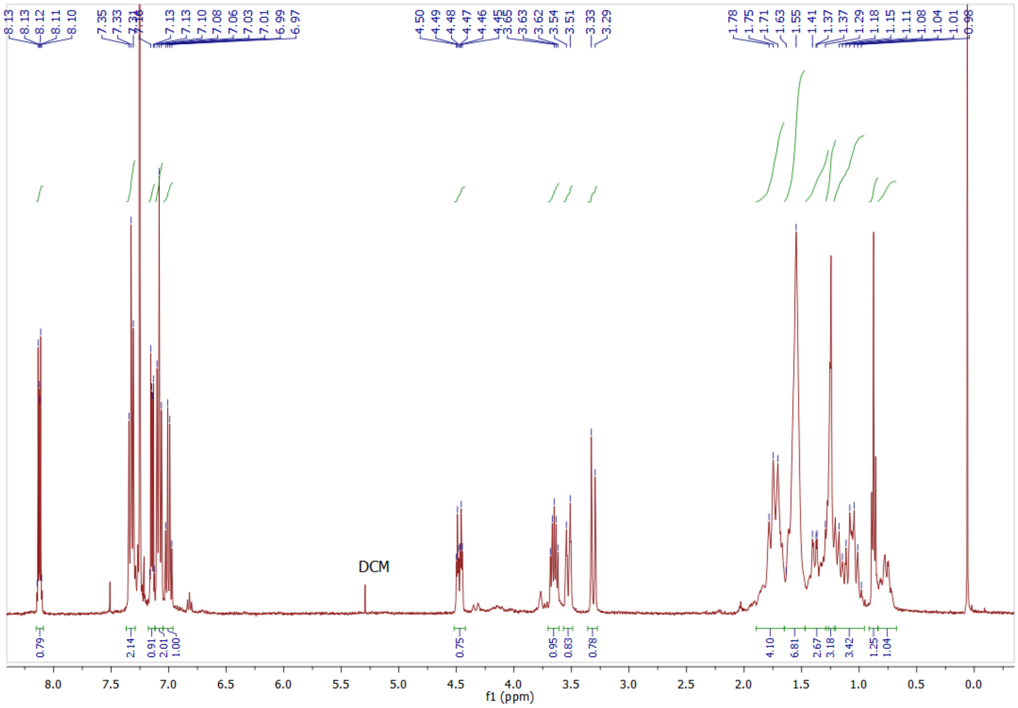

Figure ESI -8. ^{1}H-NMR spectra (400 MHz, $CDCl_3$ solution) of complex [Fe(μ-bdt)($P^{Cyc}{}_2N^{Ph}{}_2$)(CO)] **3c** (Cyc = *cyclo*-hexyl).

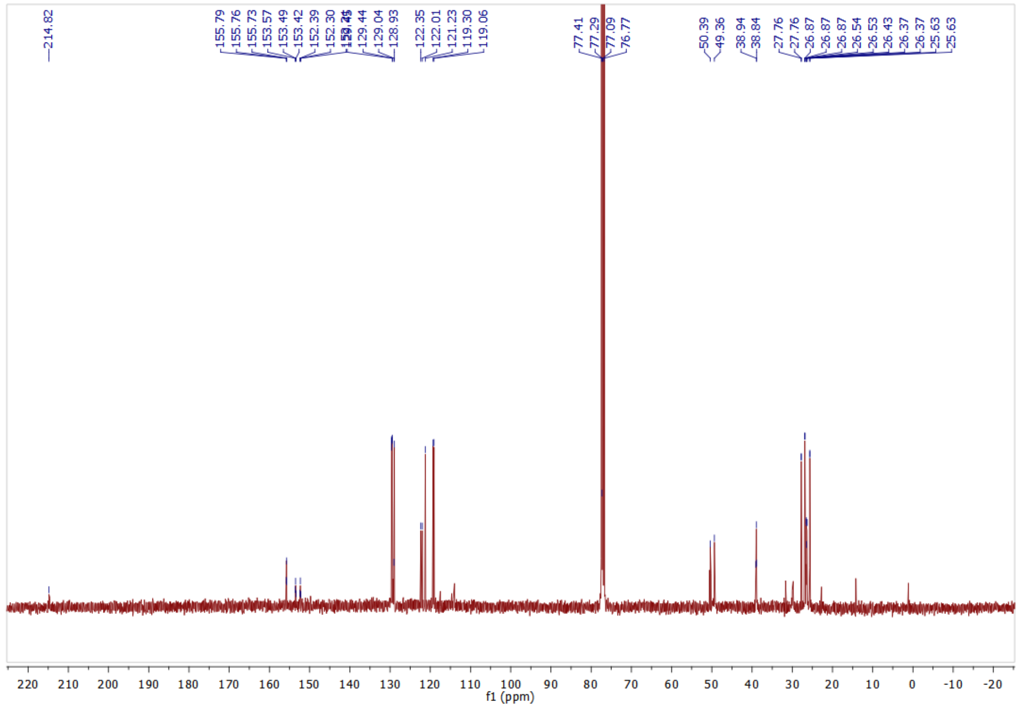

Figure ESI -9 $^{13}C\{^1H\}$-NMR spectrum (75.5 MHz, $CDCl_3$ solution) of complex [Fe(μ-bdt)($P^{Cyc}{}_2N^{Ph}{}_2$)(CO)] **3c** (Cyc = *cyclo*-hexyl).

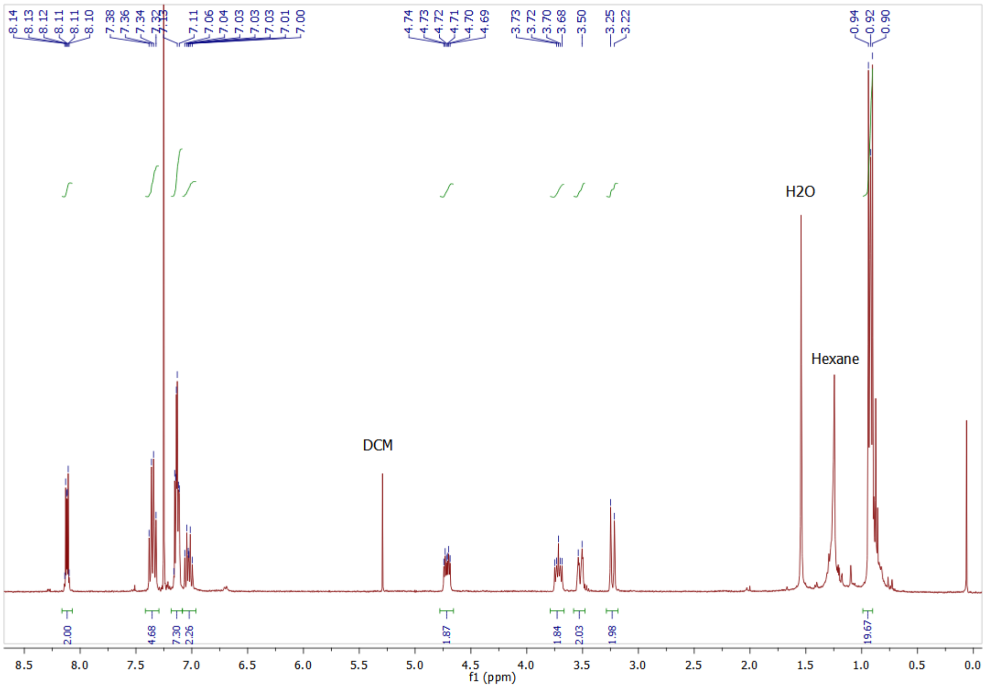

Figure ESI -10. ^{1}H-NMR spectra (400 MHz, $CDCl_3$ solution) of complex [Fe(μ-bdt)($P^{tBu}{}_2N^{Ph}{}_2$)(CO)] **3d** (tBu = *tert*.-butyl).

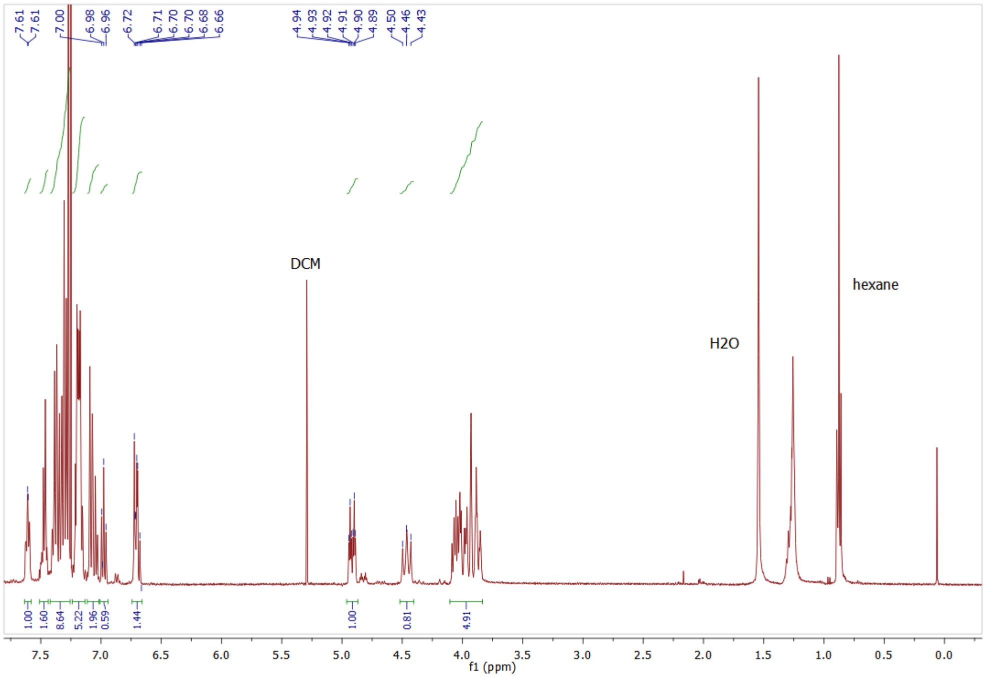

Figure ESI -11. ^{1}H-NMR spectra (400 MHz, $CDCl_3$ solution) of complex [Fe(μ-Cl_2bdt)($P^{Ph}{}_2N^{Ph}{}_2$)(CO)] **4a** (μ-Cl_2bdt = 3,6-dichloro-1,2-benzenedithiolate).

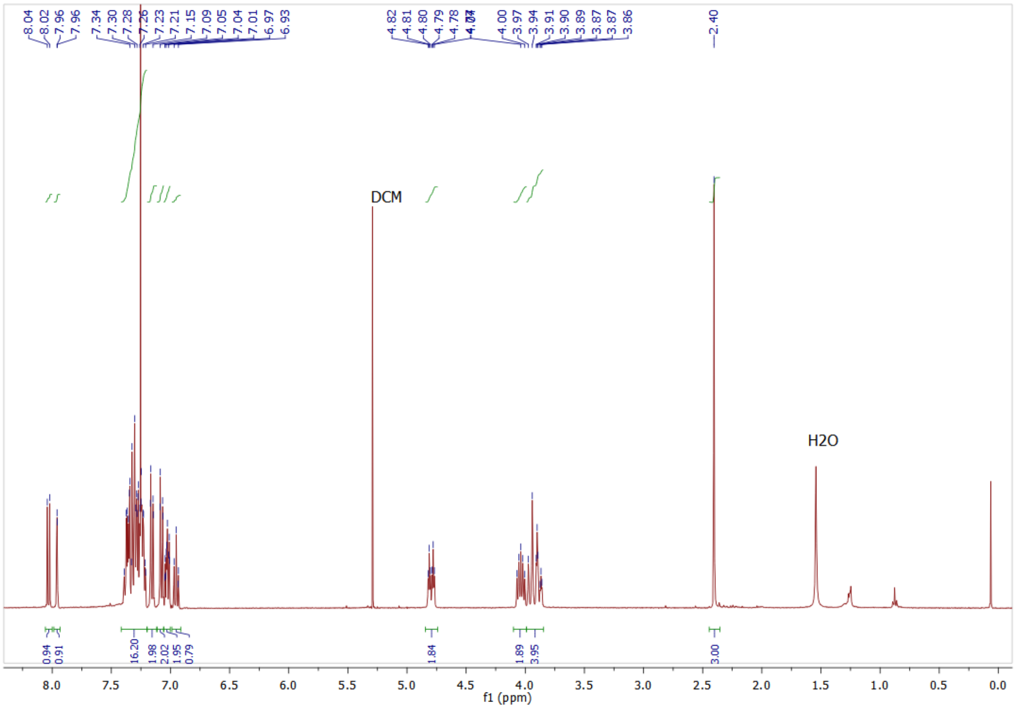

Figure ESI -12. ^{1}H-NMR spectra (400 MHz, $CDCl_3$ solution) of complex[Fe(μ-Mebdt)($P^{Ph}{}_2N^{Ph}{}_2$)(CO)] **5a** (μ-Mebdt = 4-methyl-1,2-benzenedithiolate).

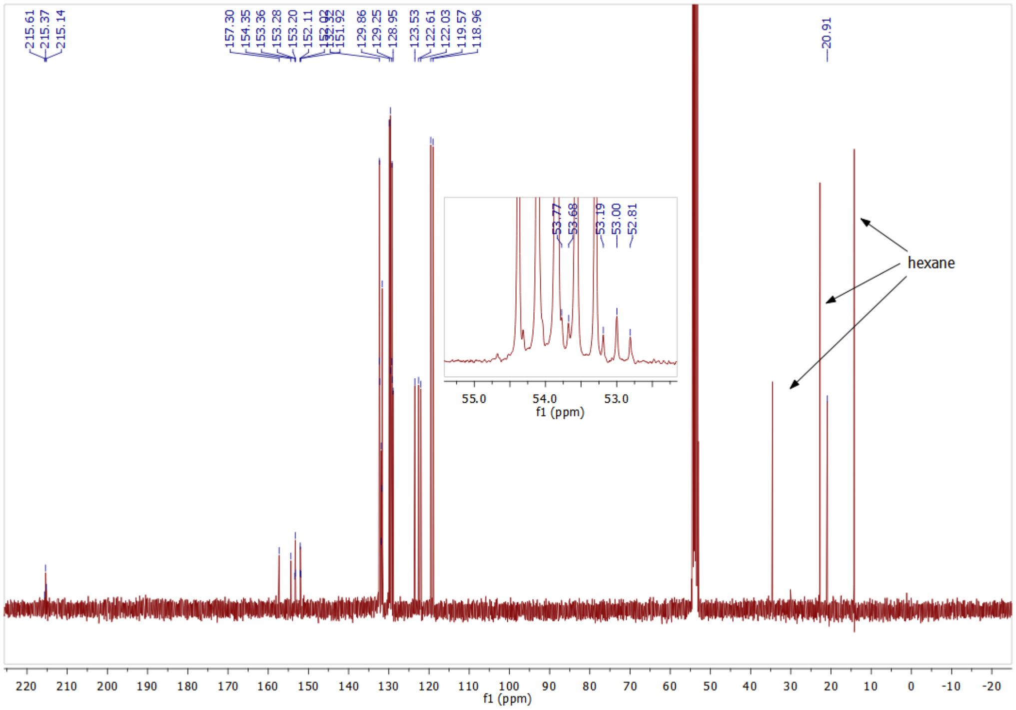

Figure ESI -13. $^{13}C\{^{1}H\}$-NMR spectrum (75.5 MHz, CD_2Cl_2 solution) of complex [Fe(μ-Mebdt)($P^{Ph}{}_2N^{Ph}{}_2$)(CO)] **5a** (μ-Mebdt = 4-methyl-1,2-benzenedithiolate).

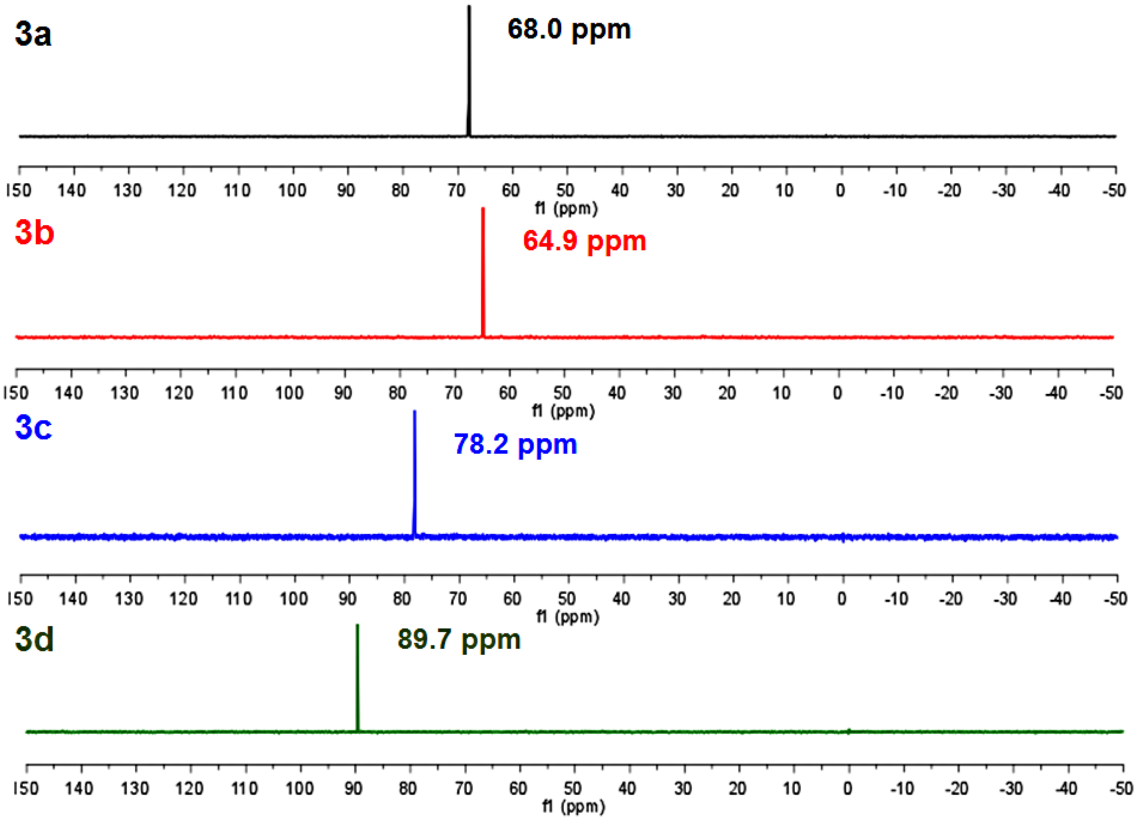

Figure ESI -14. Comparison of $^{31}P\{^1H\}$-NMR spectra (161.8 MHz, $CDCl_3$) of the complexes **3a-d.**

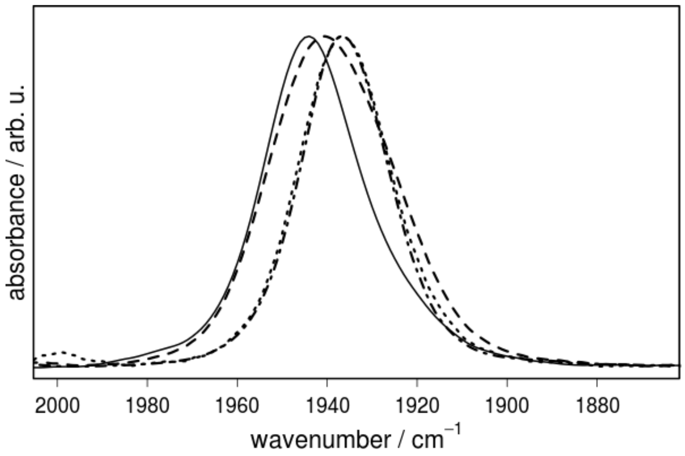

Figure ESI -15. Normalized IR spectra of **3a** (line), **3b** (dashed), **3c** (dotted) and **3d** (dash-dotted) in dichloromethane in the region of the carbonyl stretching vibrations.

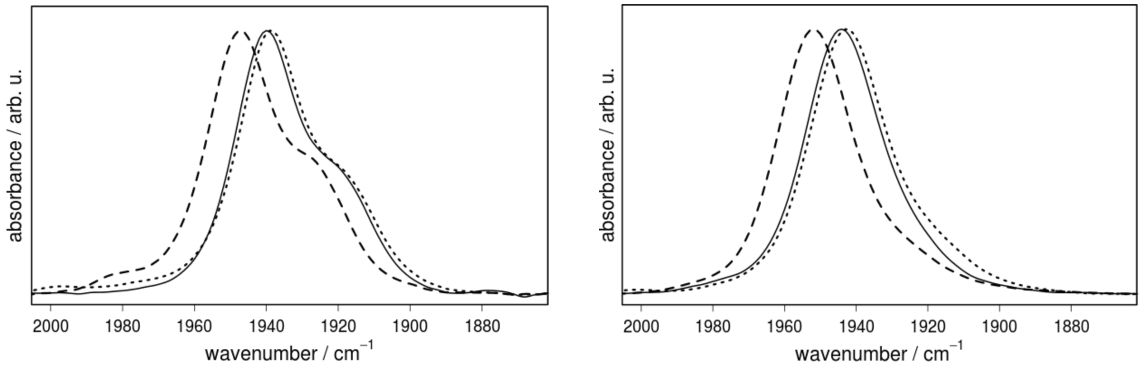

Figure ESI -16. Normalized IR spectra of **3a** (line), **4a** (dashed) and **5a** (dotted) in acetonitrile (left) and in dichloromethane (right) in the region of the carbonyl stretching vibrations.

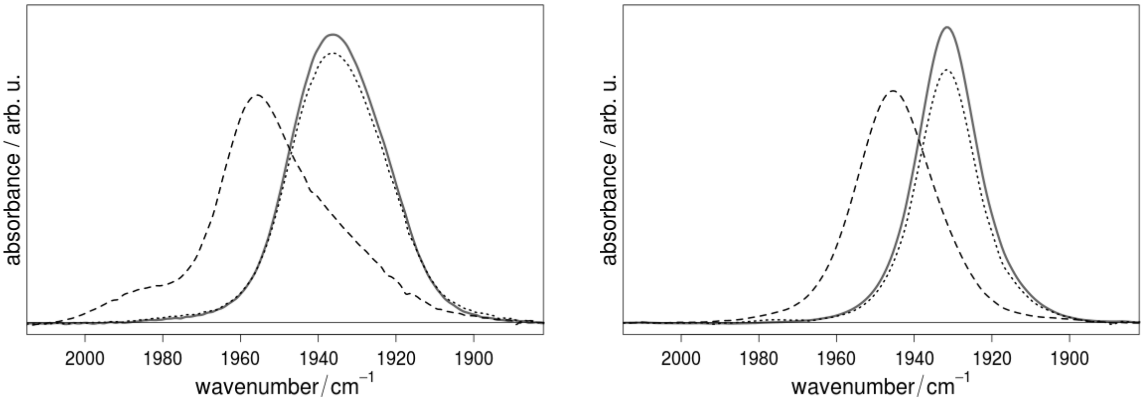

Figure ESI-17. IR spectra in the region of the carbonyl stretching vibrations of **3b** (left) and **3c** (right) before (line) and after the addition of 5 eq. trifluoromethanesulfonic acid (dashed). Both protonated complexes were successfully deprotonated with 5eq triethylamine. Conditions: acetonitrile, ambient temperatures.

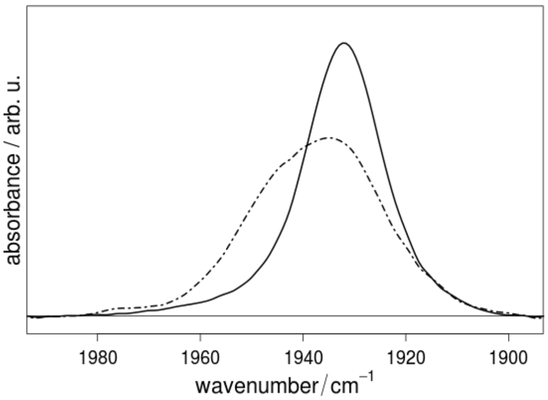

Figure ESI -18. IR spectra in the region of the carbonyl stretching vibrations of **3d** before (line) and after the addition of 43 eq. p-toluenesulfonic acid (dashed). Conditions: acetonitrile, ambient temperatures.

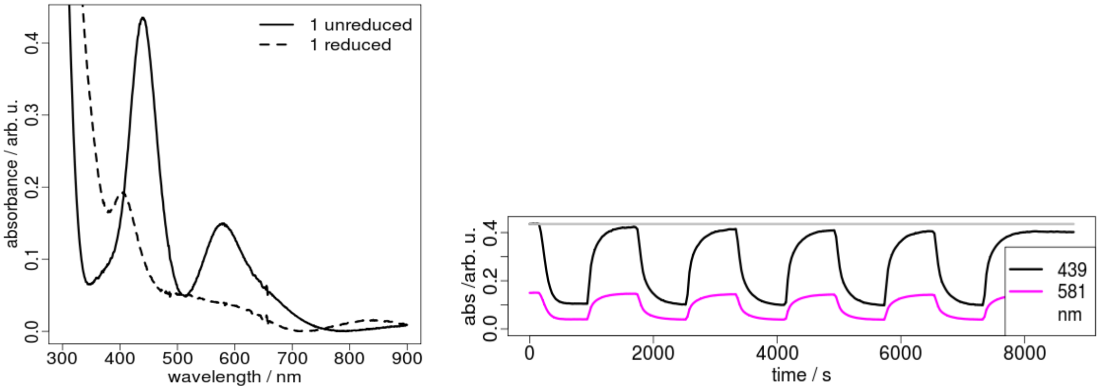

Figure ESI -19. UV/vis-Spectro-electro chemistry (SEC) spectra (left) recorded during reduction of a 1.0 mM solution of **3a** in acetonitrile solution under inert conditions. UV/vis absorbance vs. time traces (right) for two selected maxima [439 (black) and 581 nm (purple)].

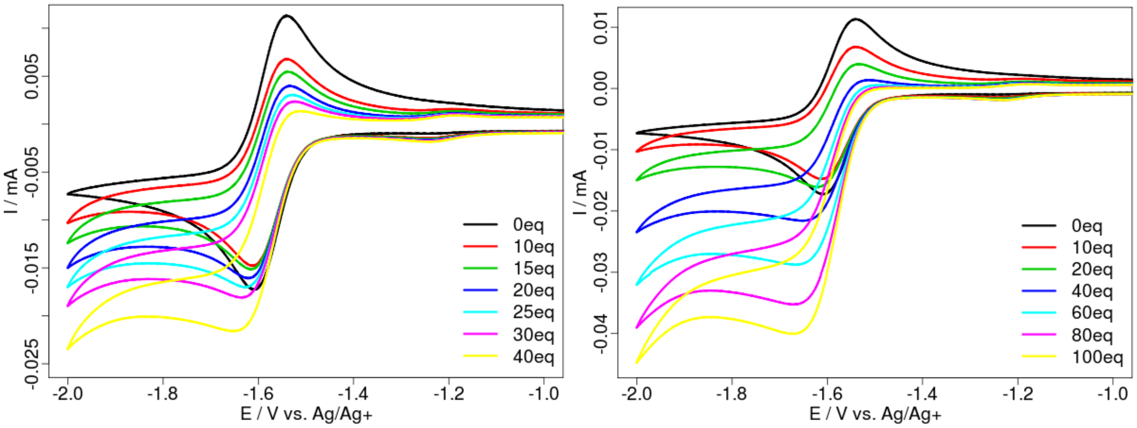

Figure ESI -20. Cyclic voltammograms of **3a** (1.0 mM) in ACN solution in the absence (black) and presence (colored curves) of increasing AcOH concentrations (left: 0-40 eq. and right: 0-100 eq.). The increase in current in the presence of acid indicates that the proton reduction is catalyzed by the iron complex. Conditions: scan rate 100 mV s^{-1}, $(Bu)_4NPF_6$ (0.1 M) as supporting electrolyte, Ag/Ag^+ reference electrode and glassy carbon working electrode.

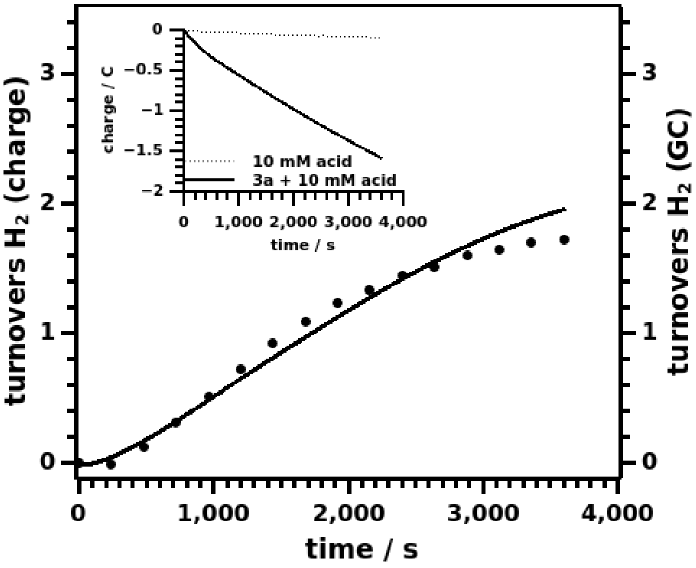

Figure ESI -21. Electro-catalytic activity of **3a**. For bulk-electrolysis experiments 6 ml of a 1 mM solution of **3a**, 0.1 M acetic acid and 0.1 M $(Bu)_4NPF_6$ in ACN were used. The reduction was carried out at -1.68 V *vs.* Fc/Fc^+. Turnovers of produced hydrogen are given as determined from the integrated current (solid line, left axis) and by *in situ* gas chromatography (dots, right axis). The inset compares the charge passed through the working electrode immersed in 10 mM acetic acid, 0.1 M $(Bu)_4NPF_6$ in ACN at an applied potential of -1.68 V *vs.* Fc/Fc^+ in presence (solid line) and absence (dotted line) of 1 mM **3a**.

Calculation of Overpotential:

A value of -70 mV vs. Fc^+/Fc was used for the thermodynamic potential of the proton/dihydrogen couple in acetonitrile. This yields a thermodynamic potential of -1.39 V vs. Fc^+/Fc for the reduction of acetic acid in acetonitrile (based on $E°[HA] = E°[H^+] – 2.3\ RT/F\ pK_a[HA]$). The corresponding overpotential at which the bulk electrolysis experiments were performed thus amounts to -290 mV (= -1.68 + 1.39 V vs. Fc^+/Fc).

Computational Details

Table ESI-2 . a) Hexacoordinate compound –pentacoordinate compound-CO + 5/2 RT. T = 298 K, 1 atm

Compound (Method)	CO ligand binding free energies[a]	
1		
BP86+D3/TZVP	-39.45	
BP86+D3/TZVP COSMO	-39.78	
B3LYP+D3/TZVP	-27.43	
B3LYP+D3/TZVP COSMO	-27.58	
2	Square pyramidal	Trigonal bi-pyramidal
BP86+D3/TZVP	-4.77	-33.21
BP86+D3/TZVP COSMO	-5.14	-26.78
B3LYP+D3/TZVP	+1.38	-18.63
B3LYP+D3/TZVP COSMO	+1.14	-11.53

Table ESI-3. a) Td-tbipy. Energy difference of Td and square pyramidal conformations of calculated pentacoordianted compexes **1**$^{-CO}$ and **2**$^{-CO}$. b) Calculated at 298 K, 1 atm

	ΔE (0 K)	ΔH	TΔS[b]	ΔG[b]
1^{-CO} (Td-tbipy)[a]				
BP86+D3/TZVP	-19.4	-18.7	+1.6	-20.3
BP86+D3/TZVP COSMO	-22.3	-22.7	+3.3	-26.0
B3LYP+D3/TZVP	-17.4	-17.4	+0.3	-17.3
B3LYP+D3/TZVP COSMO	-19.7	-21.4	+0.5	-21.9
2^{-CO} (Td-tbipy)[a]				
BP86+D3/TZVP	-27.5	-27.4	+1.0	-28.4
BP86+D3/TZVP COSMO	-27.1	-26.2	+4.6	-21.6
B3LYP+D3/TZVP	-18.3	-19.7	+0.3	-20.0
B3LYP+D3/TZVP COSMO	-18.0	-17.2	+4.5	-12.7

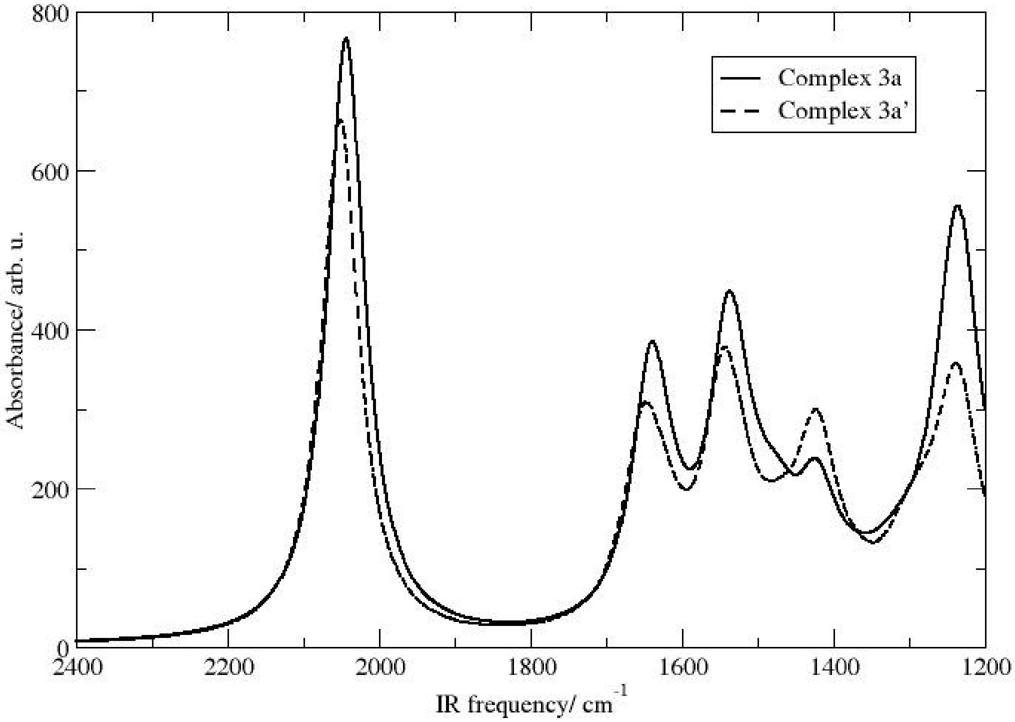

Figure ESI-22. Comparison of calculated vibrational spectra of **3a** and **3a'** between 1200 and 2400 cm^{-1}. (B3LYP+D3/TZVP results)

Table ESI-4. Energy, enthalpy and Gibbs energy differences of **3a'** and **3a** given in kcal mol^{-1}. Thermodynamic corrections apply to 298.15 K and p = 1 atm.

3a'-3a [kcal mol^{-1}]	ΔE (0 K)	Δ thermal corrections	ΔH	TΔS	ΔG
BP86+D3/TZVP	-4.09	+1.35	-2.75	+1.77	-4.52
BP86+D3/TZVP COSMO	-5.32	+1.16	-4.16	+2.41	-6.57
B3LYP+D3/TZVP	-3.63	+1.05	-2.59	+2.71	-5.30
B3LYP+D3/TZVP COSMO	-5.12	+0.13	-5.25	+1.54	-6.79

Table ESI-5. CO ligand binding affinities of complex **3a'**

3a'	CO ligand binding free energies in kcal mol^{-1}
BP86+D3/TZVP	+1.57
BP86+D3/TZVP COSMO	+0.52
B3LYP+D3/TZVP	+4.88
B3LYP+D3/TZVP COSMO	+3.91

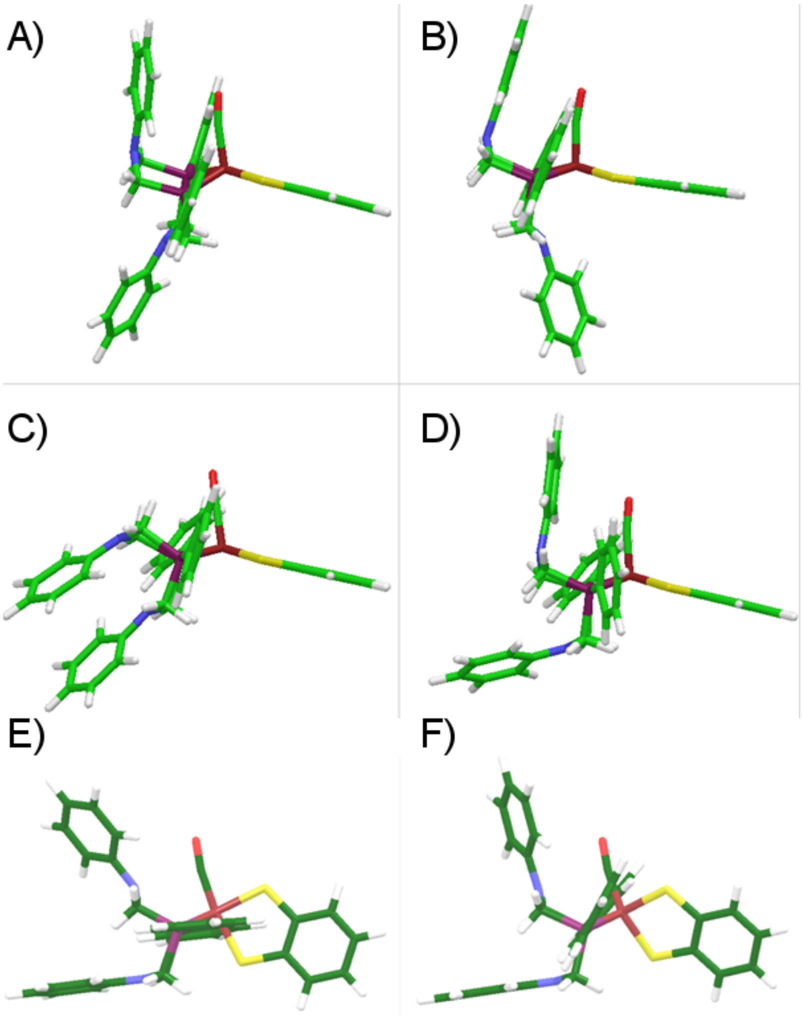

Figure ESI-23. Depiction of calculated structures of complex **3a**. BP86+D3/def2-TZVP COSMO (acetonitrile). A) **3a'**$_{\mathbf{endo/exo\text{-}ph}}$ B) **3a'**$_{\mathbf{endo/endo}}$ C) **3a'**$_{\mathbf{exo/exo}}$ D) **3a'**$_{\mathbf{endo/exo\text{-}lp}}$ E) **3a**$^{\mathbf{cryst}}_{\mathbf{endo\text{-}lp}}$ F) **3a**$^{\mathbf{cryst}}_{\mathbf{endo\text{-}ph}}$

Table S6. Relative energies of complex **3a** and the corresponding CO stretching vibrations. BP86+D3/def2-TZVP/COSMO(acetonitrile).

	C=O freq v/cm-1	ΔΔG (298K, 1atm)/kcal mol-1
3a'$_{\mathbf{endo/exo\text{-}ph}}$	1886	+ 3.0
3a'$_{\mathbf{endo/endo}}$	1922	+ 2.8
3a'$_{\mathbf{exo/exo}}$	1877	+ 2.4
3a'$_{\mathbf{endo/exo\text{-}lp}}$	1900	+1.7
3a$^{\mathbf{cryst}}_{\mathbf{endo\text{-}lp}}$	1887	0.0
3a$^{\mathbf{cryst}}_{\mathbf{endo\text{-}ph}}$	1899	1.4

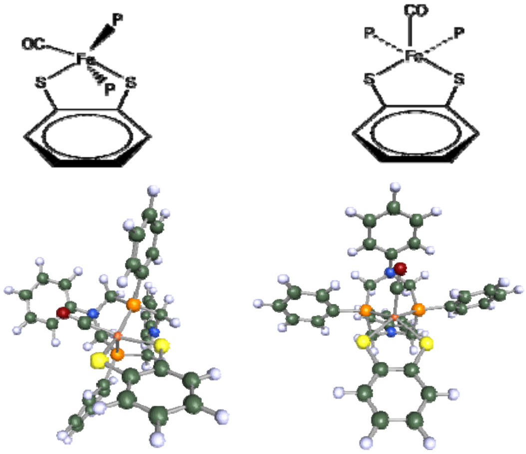

Figure ESI-24. Conformations of complex **3a**, as found in the crystal **3a**$^{\mathbf{cryst}}$ (left) and the square-pyramidal **3a**' (right) which is 5 kcal mol^{-1} lower in energy determined by B3LYP+D3/TZVP calculations.

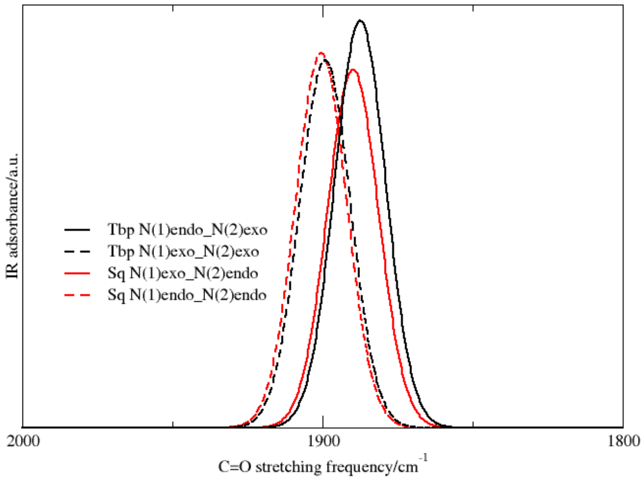

Figure ESI-25. Superposition of calculated vibrational spectra (CO strech region) of **3a**$_{\text{endo-lp}}$ (red, dashed), **3a**$_{\text{endo-ph}}$ (red, solid) and **3a'**$_{\text{endo-lp}}$, (black, dashed) **3a'**$_{\text{endo-ph}}$ (black,solid). Results from BP86+D3/def2-TZVP COSMO (acetonitrile) calculations.

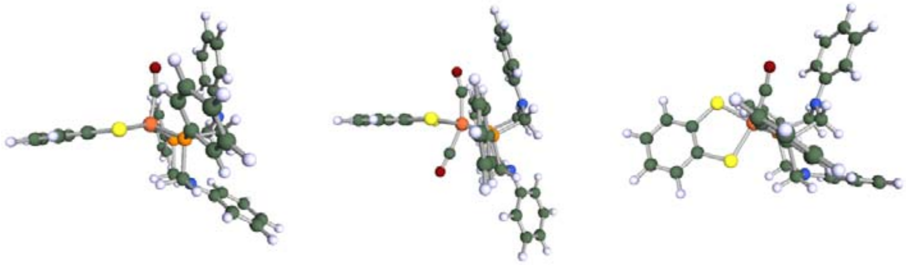

.

Figure ESI-26. Potential CO coordination to penta coordinate complexes. **3a’**(left), **3a’**+CO(middle), **3a**^{cryst} (right). Note that CO coordination is not possible in **3a**^{cryst}.